RZ 3618 (# 99628) 07/25/05
Physics 11 pages

Research Report

Studying the Effects of Nitrogen and Hafnium Incorporation into the SiO_2/Si(100) Interface with Replica-exchange Molecular Dynamics and Density-functional-theory Calculations

W. Andreoni, A. Curioni, D. Fischer, S. Billeter, and C.A. Pignedoli

IBM Research GmbH
Zurich Research Laboratory
8803 Rüschlikon
Switzerland

LIMITED DISTRIBUTION NOTICE

This report has been submitted for publication outside of IBM and will probably be copyrighted if accepted for publication. It has been issued as a Research Report for early dissemination of its contents. In view of the transfer of copyright to the outside publisher, its distribution outside of IBM prior to publication should be limited to peer communications and specific requests. After outside publication, requests should be filled only by reprints or legally obtained copies of the article (e.g., payment of royalties). Some reports are available at http://domino.watson.ibm.com/library/Cyberdig.nsf/home.

IBM Research
Almaden · Austin · Beijing · Delhi · Haifa · T.J. Watson · Tokyo · Zurich

Studying the Effects of Nitrogen and Hafnium Incorporation into the SiO_2/Si(100) Interface with Replica-exchange Molecular Dynamics and Density-functional-theory Calculations

WANDA ANDREONI *, ALESSANDRO CURIONI, DOMINIK FISCHER, SALOMON R. BILLETER, CARLO A. PIGNEDOLI
IBM Research, Zurich Research Laboratory, 8803 Rüschlikon, Switzerland

Abstract. By combining large-scale classical molecular dynamics simulations, the replica exchange method and *ab initio* calculations, we have studied how the incorporation of nitrogen and hafnium affects the physical and chemical properties of the silicon/silicon dioxide interface. This paper focuses on the determination of the structure of the SiO_2/Si(100) interface and on the changes induced on its microscopic characteristics by nitrogen introduced at different concentrations (in the range from 1% to 14%). Characteristic Si- and O-centered defects are observed and in particular N-centered defects—also unforeseen ones. Additional defects emerging after hydrogenation are also considered. The effects of silicon replacement with hafnium atoms at various levels in the interface region are also studied, both in the stoichiometric and substoichiometric oxide.

1. Introduction

The motivation for the research we present here lies in the ever growing need for a better understanding of the microscopic structure of nanoscale interfaces between silicon and oxides such as SiO_2 and SiON, currently used in CMOS devices, or HfO_2 , which is considered for application in the near future (for recent reviews, see e.g. Refs. 1,2,3). A large amount of data and knowhow has been accumulated over the years, both from experiment and from calculations of diverse levels of sophistication, on SiO_2 and its interfaces with silicon. However, a few outstanding questions are still open concerning the physical behavior of this material, which are related to the mechanisms responsible for the dielectric breakdown when the thickness is reduced to less than 2 nm. The investigation of microscopic changes induced by nitridation of films in the sub-nanometer scale is more recent and apparently less clearly understood. Concerning the understanding of HfO_2 /Si interfaces, progress continues to be made daily, but it is still unclear whether (or to

what extent) heavy-metal atoms penetrate the silicon substrate after deposition.

Our investigation[4] is based on computer simulations of SiO_xN_y/Si(100) interfaces (with stoichiometric composition $y = 2(2\text{-}x)/3$ and also nonstoichiometric with moderate oxygen excess) for a nitrogen content $\xi = y/(x + y) = 0$ (pure SiO_2), ~1, 3, 6 and ~14%. Hafnium atoms were also incorporated with concentration x ranging from ~1 to ~5% in replacement of silicon atoms at various positions in the dioxide as well as in the suboxide region. The determination of the structure of the SiO_xN_y/Si(100) interfaces was made using the Molecular Dynamics (MD) driven replica-exchange method[5] which greatly enhances the sampling rate of the configurations and also allows one to monitor the system behavior at different temperatures. In these MD simulations the interatomic interactions were described with DFT-derived potentials[6]. In particular, some unforeseen defect configurations are found which are N-centered and increase with N content. DFT calculations of these defect configurations and others with added hydrogen (in the neutral and positively charged states) were performed on smaller samples. DFT calculations are also performed to characterize the changes induced by hafnium replacing silicon atoms of different oxidation states, at low concentration, and to determine the relative thermodynamic stability of the corresponding configurations as well as their electronic structure.

2. Computational scheme

2.1. METHODS

In the simulations we describe in the following sections, both *ab initio* approaches and classical potentials for molecular dynamics simulations were adopted.

The *ab initio* calculations were performed within the framework of density-functional theory using the Perdew-Burke-Erzernhof[7] approximation for the gradient-corrected exchange-correlation energy functional, norm-conserving angular-momentum dependent pseudopotentials[8] to represent the interaction of the valence with core electrons, and plane waves as basis set for the expansion of the wavefunctions up to a 80 Ry cutoff[9]. For SiON(H) systems we refer to our results on the structural and dielectric properties of bulk phases[10], which document their validity. In the case of hafnium, the validity of the pseudo-potential scheme (with f-electrons considered frozen in the core) was also verified on bulk properties of Hafnia[11].

The classical potentials for Si, O, N and H—which are coordination-dependent and are based on an extension of the Tersoff potential for silicon[12] —

were consistently derived from fitting to DFT-PBE results[9] that we have obtained for a relatively large set of compounds and configurations[6] via simultaneous energy and force matching[13]. In particular, an additional number of tests were made against DFT-PBE results, on structural characteristics, vibrational spectra, and the energetics of defects.

In the REMD simulations, 128 replicas, distributed over temperatures ranging from 50 to 1500 K, were explored for each system and each one for a period of time ranging from 2.5 to 3.1 nsec.

2.2. MODEL SYSTEMS

The atomistic models used to represent the interfaces consisted of 3D periodically repeated slabs in which the oxide was sandwiched between two ~8-Å-thick silicon multilayers so as to prevent spurious truncation effects. Indeed this configuration is physically interesting because it can be considered to represent the environment of the dielectric film in MOSFET devices, where it is sandwiched between silicon and polysilicon.

In classical MD simulations, the samples contained 2088 atoms, the global thickness of the oxide corresponded to 18–20 Å, and the periodically repeated cell had dimensions 32.54 Å × 32.54 Å × 33.70 Å. In the DFT calculations, the samples contained 522 atoms, and were obtained by cutting the original model so as to reduce the dimensions of the unit cell to 16.27 Å × 16.27 Å × 33.70 Å.

3. Results

3.1. SiO_2/Si(100)

Simulations of this interface were aimed at providing a realistic atomistic model on which one could investigate how its physical properties can be modified by the inclusion of hetero-atoms, depending on their nature and on their concentration. In previous studies, also the most advanced ones to-date[14,15], structural models of SiO_2/Si(100) were generated so as to represent some empirical data before-hand. Clearly this type of approach does not offer the flexibility necessary for our purposes. As discussed in Sect. 2, in our search for a thermodynamically stable structure we do not enforce any constraint on the atomic coordinates and make use of the REMD method to efficiently sample the configurational space. Here we briefly review the main results of our research that are discussed in more detail in Ref. 4.

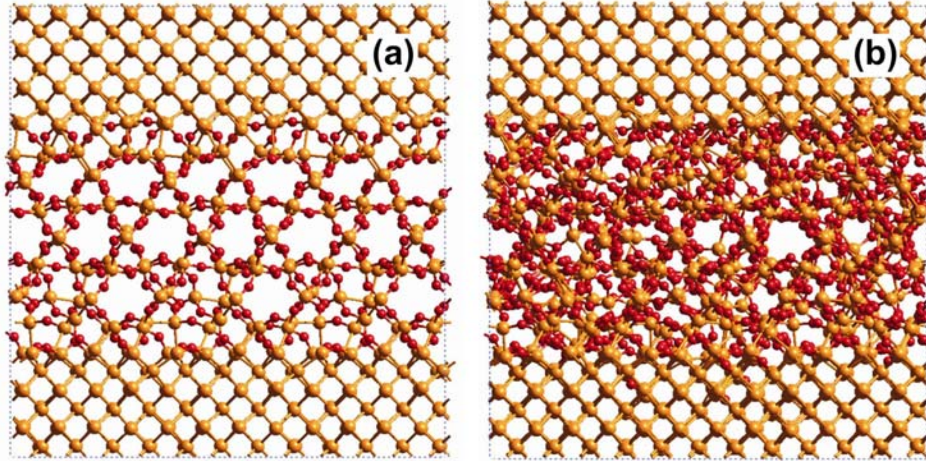

Figure 1. (a) Initial configuration (abrupt interface) and (b) snapshot of a low-temperature configuration resulting from our simulations.

Our REMD simulations start from an abrupt interface (see Fig. 1(a)) with a moderate excess of oxygen atoms randomly distributed on the silicon back-bonds. The system is observed to progressively undergo a strong rearrangement as can be seen in Fig. 1(b). In particular, the distribution of the substoichiometric oxide species rapidly establishes itself. Figure 2(a) shows the time evolution of the relative concentrations of silicon atoms in oxidation states Si^{+n} with n = 1, 2, and 3, averaged over all replicas comprised in the temperature range 200–400 K. The statistical average at room temperature corresponds to ratios Si^{+2}/Si^{+1} = 1.4 and Si^{+3}/Si^{+1} = 1.6. Values derived from fitting to experimental data exhibit a non-negligible scattering (e.g. from 1;1 [16] to 2;2 [17] to 2;3 [19,19]), and seem to depend on the type of experiment as well as on a number of factors related to the sample itself, such as film thickness[17] and growth conditions[20]. The Si^{+1} atoms are generally indicated as the minority species and also the ones whose distribution is less affected by either thickness or temperature. Still comparison with experiment cannot be straightforward unless a step forward is made in the calculations and on the basis of a structural model, theoretical photoemission spectra are determined. The average distribution of silicon atoms we calculate at room temperature is shown in Fig. 2(b) for all five oxidation states. The Si^{+1} component slightly penetrates into the substrate as a consequence of oxygen diffusion, and the Si^{+3} component protrudes into the bulk SiO_2. Indeed Si^{+3} species have been observed to have a relatively higher extension, from the earliest X-ray photoemission study[21] to more recent angle-resolved Si 2p photoemission[19]. One can try to estimate the width of the

suboxide from Fig. 2(b), for example as the distance between the first maximum of the Si^{+1} distribution and the first maximum of the Si^{+4} one, which amounts to ~6 Å. A variety of measurements on films of different thickness (see e.g. Refs. 19, 22, 23) indicates a value closer to 5 Å. Again the correspondence between specific experimental observation and the outcome of a profile plot is not a one-to-one correspondence.

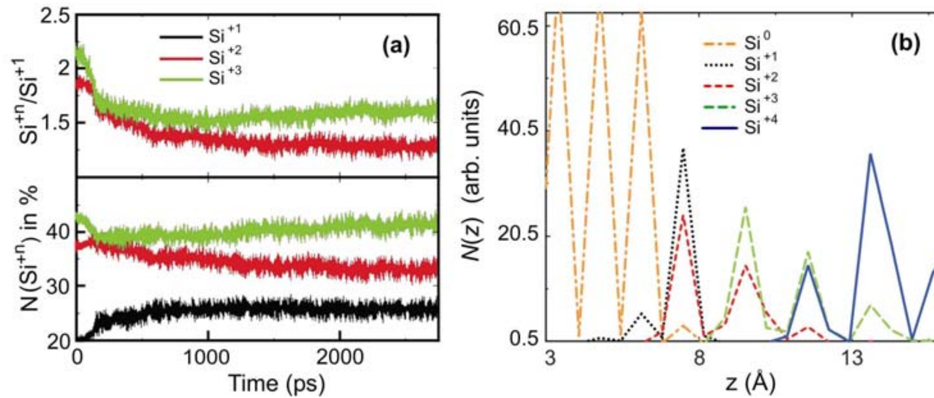

Figure 2. (a) Time variation of the distribution of silicon atoms in sub-oxidized states, and (b) average density profile of all states calculated at room temperature (see text).

In spite of the strong rearrangement of the atomic positions, a pattern rapidly established itself on the surface layer, similar to that observed in cristobalite. This feature corresponds closely to high-resolution electron microscopy (HREM) [24] observations on very thin films and also by XRD[25] on thicker samples. The formation of this ordered cristobalite-like pattern in the proximity of the substrate drives an increase in the atom density over the transition region: on average, we calculate a 10% enhancement over 6 Å towards the Si layers. This fact is consistent with – although not directly comparable to – the observation of a "high-density layer" of 10 Å in the transition region of thicker films (40 Å)[26].

Unlike previous models that were constrained to be defect-free,[15,27] our results show the presence of the characteristic defects of this system, namely, under-coordinated Si and over-coordinated O atoms, the latter having maximum concentration in the proximity of silicon. Being forcedly diamagnetic, no direct comparison with ESR experiments can be made. As expected, their average density (taken over the 200–600 K temperature range) is higher than what ESR indicates for real systems, namely, by a factor of 2 to 10, depending on the reference system (see e.g. Ref. 28).

While detailed comparison with experiment awaits for simulations of the processing of the material, such as to generate a structural model similar to thermally grown silicon oxide, the results here obtained provide a physically sound ground on which the effects of incorporation of heteroatoms can be studied.

3.2. SiON / Si(100)

Recently we have undertaken an extensive investigation of the interfaces of oxynitrides with silicon. For comparison with a number of previous studies (see e.g. Ref. 29, 30) we refer to Ref. 31 . In this section, we describe only our most salient and novel findings.

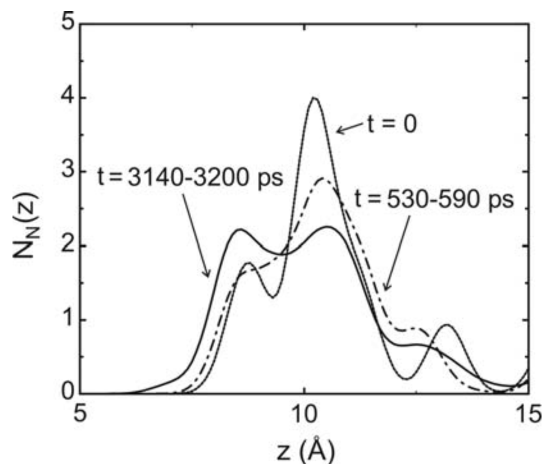

Figure 3. Nitrogen profile calculated for the ξ = 3% sample at room temperature.

Starting from a low-temperature configuration found above for the bare interface, we have incorporated nitrogen atoms for concentrations corresponding to ~1, ~3, ~6 and ~14% of nitrogen content ξ. In the initial configurations the oxygen atoms were replaced by nitrogen atoms throughout the system but according to a given profile. However no constraint was enforced on the atomic coordinates. Figure 3 shows how the nitrogen profile changed over time for the ξ = 3% sample. The tendency of nitrogen to localize itself closer to silicon is apparent. That important changes take place during the REMD simulations is evidentiated by the transformation of the large majority of nitrogens from two- to three-fold coordinated. In Fig. 4 we have plotted the change with time of the number of defects for all the species observed in the ξ = 6% sample, which is however representative of all cases calculated. As expected three-fold coordinated nitrogen atoms (not shown in the figure) evolve so as to form the stable

network of the nitridated interface at the expense of the two-folded coordinated species that dramatically decrease. This is accompanied by the manifest increase of the number of under-coordinated silicon atoms, while the amount of over-coordinated oxygen does not seem to be affected by the reconstruction of the structure. Interestingly a tiny amount of unforeseen 4-fold coordinated nitrogen (Si_4-N) emerges. With DFT calculations we have verified that this result was not an artifact of the classical potential scheme.

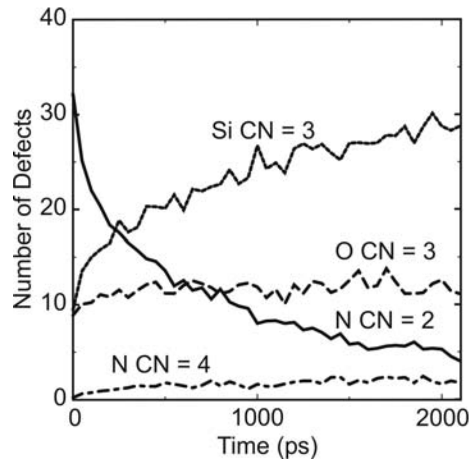

Figure 4. Time evolution of the number of the various characteristics defects observed in the ξ = 6% sample at room temperature.

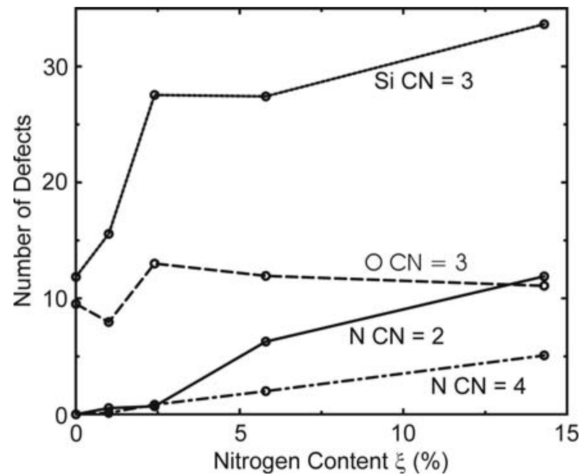

Figure 5. Number of defects as a function of nitrogen content, at room-temperature.

With increasing nitrogen content (see Fig. 5) we observe that unlike over-coordinated oxygen atoms, the density of both nitrogen- and silicon-centered defects also increases. In particular this is true for the 4-fold coordinated nitrogen. We notice that contrary to the case of under-coordinated silicon (the majority defect) that can be passivated by hydrogenation, over-coordinated nitrogen cannot be removed with this procedure.

Given the well-known high stability of positively charged 4-fold-coordinated nitrogen (e.g. in ammonia salts), the nitrogen configurations here detected might form positively charged defects that can act either as fixed charges or electron traps. Moreover, positively charged 4-fold-coordinated nitrogen could also be generated by hydrogen sticking at network 3-fold coordinated nitrogen (Si_3-N) and also at formerly hydrogen passivated 2-fold coordinated nitrogen. DFT calculations of the binding affinity of hydrogen, both neutral and ionized, were performed. In particular binding affinities for the Si_3-N species are 1 eV for H and 4.1 eV for H^+, only slightly lower than those for Si_2-O in silica (1.1 and 4.4 eV, respectively). Interestingly, the formation of Si_3-NH^+ in plasma-nitridized SiON/Si(100) systems has recently been invoked[32] as a possible ESR-inactive interface defect which can contribute to near-bias temperature stress (NBTS). A detailed investigation of N-induced defects is currently underway using first-principles calculations with the aim of determining the mechanisms by which they can contribute to negative-bias temperature instability (NBTI) and affect electron mobility.

3.3. Hf AT SiO_2/Si(100)

The effects induced by incorporation of hafnium in the SiO_2/Si(100) interface were investigated[11] for hafnium concentrations of 1% and 5%. Only configurations were studied in which hafnium enters as a substitutional impurity. As reported in Table 1, hafnium strongly prefers to replace a silicon atom in the dioxide rather than in the suboxide region. This is consistent with the fact that hafnium-rich silicates are stable in structures with high coordination (6–7) and in this system the tetrahedral coordination is the highest possible. The change of local environment, compared to silicon, amounts to a 0.2–0.3 Å expansion of the bond lengths, which is a sign of localized strain. Unlike silicon-silicon distances, hafnium-silicon distances shrink with decreasing number of coordinating oxygens.

Table 1 Energy and bond lengths (in Å) of interface configurations with hafnium replacing one silicon atom of a given oxidation state (1% hafnium). Energies are referred to the lowest state that corresponds to hafnium located in the dioxide region. Si-Si and Si-O distances are calculated in the interface without hafnium.

Oxidation State	Energy (eV)	d_{av} Hf-O	d_{av} Si-O	d_{av} Hf-Si	d_{av} Si-Si
+4	0	1.92	1.64	–	–
+3	1.2	1.92	1.65	2.65	2.36
+2	2.5	1.85	1.67	2.57	2.36
+1	3.1	1.81	1.67	2.57	2.36

Although hafnium is unlikely to penetrate into the suboxide according to mere thermodynamics grounds, it is interesting to consider the modifications that such an event would involve. Our most interesting observation refers to the case of the replacement of silicon in the +1 state. An increment of the electron density at the Fermi edge emerges already for a hafnium content of 1% and is further enhanced at 5% as shown in Fig. 6(b). These new states are hafnium-related states and are delocalized in the proximity of the silicon substrate, as illustrated in Fig. 6(a). This scenario might be considered as the precursor of a metallic interfacial layer.

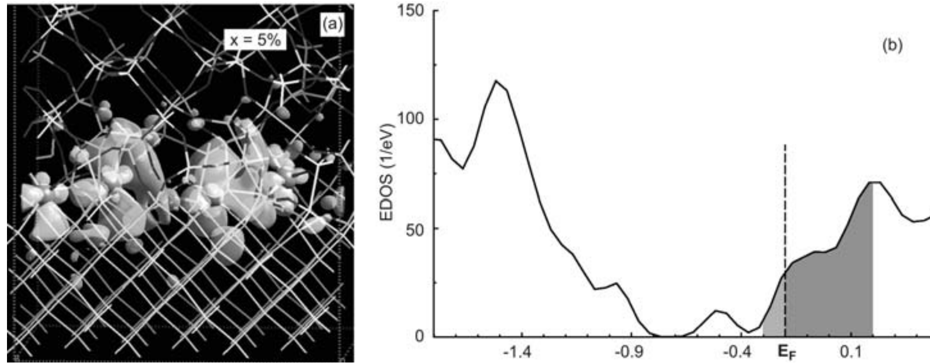

Figure 6. SiO_2/Si(100) with Hf replacing Si^{+1} atoms in the suboxide at a concentration of 5%. (b) Density of electron states around the Fermi level and (a) a representative isosurface of the corresponding probability density. Circles denote hafnium atoms.

An early attempt[33] to calculate the effects of the incorporation of hafnium on different layers of the interface also concluded that the metal atom prefers to be located in bulk-like SiO_2. However a direct comparison cannot be made with our results, because the configurations considered for the substitutional hafnium

did not differ in its oxidation state. Indeed that model did not account for a substoichiometric region. The interface, whose unit cell had lateral dimentions of the silicon unit cell, was abrupt (β-quartz SiO_2 with an oxygen bridge aimed at eliminating interface states due to unsaturated bonds) so that only Si^{+2} was present as sub-oxidized species.

4. Conclusions

We believe that by combining the accuracy of the DFT method and the power of REMD simulations of large-scale systems, real progress can be made in the understanding of complex interfaces like those of SiON and high-k oxides with silicon. The results briefly surveyed above are intended to be only the beginning of a new and systematic approach to the study of their structural and electronic properties, and in particular of defects introduced during material processing .

*To whom correspondence should be addressed.

References

1. J. Robertson, Europ. Phys. J. Appl. Phys. 28, 265-291 (2004).
2. A. Pasquarello and A. M. Stoneham, J. Phys.: Condens. Matter 17, V1-V5 (2005).
3. A. M. Stoneham, J. L. Gavartin and A. L. Shluger, J. Phys.: Condens. Matter S2027-S2049 and references therein.
4. D. Fischer, A. Curioni, S.R. Billeter, and W. Andreoni, preprint, submitted for publication.
5. Y. Sugita and Y. Okamoto, Chem. Phys. Lett. 314, 141 (1999).
6. S. R. Billeter, A. Curioni, D. Fischer, and W. Andreoni, preprint, submitted for publication..
7. J. P. Perdew, K. Burke, and M. Ernzerhof, Phys. Rev. Lett. 77, 3865 (1996).
8. N. Troullier and J. L. Martins, Phys. Rev. B 43, 1993 (1991).
9. These calculations used the CPMD code: CPMD Copyright IBM Corp 1990-2005; Copyright MPI für Festkörperforschung Stuttgart 1997-2001; see http://www.cpmd.org.
10. D. Fischer, A. Curioni, S.R. Billeter, W. Andreoni, *Phys. Rev. Lett.* 92, 236405 (2004).
11. C. A. Pignedoli, A. Curioni and W. Andreoni, preprint, submitted for publication.
12. J. Tersoff, Phys. Rev. B 37, 6991 (1988).
13. F. Ercolessi and J. B. Adams, Europhys. Lett. 26, 583 (1994); F. P. Tanguey and S. Scandolo, J. Chem. Phys. 117, 8898 (2002).
14. A. Pasquarello, M. S. Hybertsen, and R. Car, Phys. Rev. B 53, 10942 (1996); R. Buczko, S. J. Pennycook, and S. T. Pantelides, Phys. Rev. Lett. 84, 943 (2000)
15. A. Bongiorno and A. Pasquarello, Appl. Phys. Lett. 83, 1417 (2003).

16. S. Miyazaki, H. Nishimura, M. Fukuda, L. Ley and J. Ristein, Appl. Surf. Sci. 113/114, 585 (1997).
17. I. Jimenez and J. L. Sacedon, Surf. Sci. 482-485, 272 (2001).
18. F. Rochet, Ch. Poncey, G. Dufour, H. Roulet, C. Guillot, and F. Sirotti, J. Non-Cryst. Solids 216, 148 (1997).
19. J. H. Oh, H. W. Yeom, Y. Hagimoto, K. Ono, M. Oshima, N. Hirashita, M. Nywa, and A. Toriumi, Phys. Rev. B 63, 205310 (2001).
20. K. T. Queeney, N. Herbots, J. M. Shaw, V. Atluri, and Y. J. Chabal, Appl. Phys. Lett. 84, 493 (2004).
21. F. J. Himpsel, F. R. McFeely, A. Taleb-Ibrahimi, J. A. Yarmoff, and G. Hollinger, Phys. Rev. B 38, 6084 (1988).
22. K. T. Queeney, M. K. Weldon, J. P. Chang, Y. J. Chabal, A. B. Gurevich, J. Sapjeta, and R. L. Opila, J. Appl. Phys. 87, 1322 (2000).
23. K. Kimura and K. Nakajima, Appl. Surf. Sci. 216, 283 (2003).
24. N. Ikarashi, K. Watanabe, and Y. Miyamoto, Phys. Rev. B 62, 15989 (2001).
25. I. Takahashi, T. Kada, K. Inoue, A. Kitahara, H. Shimazu, N. Tanaka, H. Terauchi, S. Doi, K. Nomura, N. Awaji, and S. Komiya, Jpn. J. Appl. Phys., Part 1, 42, 7493 (2003); N. Awaji, Y. Sugita, Y. Horii, and I. Takahashi, Appl. Phys. Lett. 74, 2669 (1999).
26. Y. Sugita, S. Watanabe, N. Awaji, and S. Komiya, Appl. Surf. Sci. 100/101, 268 (1996).
27. Y. Tu and J. Tersoff, Phys. Rev. Lett. 84, 4393 (2000).
28. L. G. Gosset, J. J. Ganem, H. J. von Bardeleben, S. Rigo, I. Trimaille, J. L. Cantin, T. Akermark, and I. C. Vickridge, J. Appl. Phys. 85, 3661 (1999); K. Kushida-Abdelghafar, K. Watanabe, T. Kikawa, Y. Kamigaki, and J. Ushio, J. Appl. Phys. 92, 2475 (2002).
29. A. A. Demkov, R. Liu, X. Zhang, and H. Loechelt, J. Vac. Sci. Technol. B 18, 2388 (2000); S. Jeong and A. Oshiyama, Phys. Rev. Lett. 86, 3574 (2001); I. Takahashi, T. Kada, K. Inoue, A. Kitahara, H. Shimazu, N. Tanaka, H. Terauchi, S. Doi, K. Nomura, N. Awaji, and S. Komiya, Jpn. J. Appl. Phys. 42, 7493 (2003)
30. G. F. Cerofolini, A. P. Caricato, L. Meda, N. Re, and A. Sgamellotti, Phys. Rev. B 61, 14157 (2000).
31. D. Fischer, A. Curioni, S. R. Billeter, and W. Andreoni, preprint, submitted for publication.
32. S. Fujieda, Y. Miura, M. Saitoh, E. Hagesawa, S. Koyama, and K. Ando, App. Phys. Lett. 82, 3677 (2003)
33. A. Kawamoto, J. Jameson, P. Griffin, K. J. Cho, and R. Dutton, IEEE Electron. Dev. Lett. 22, 14 (2001).